Electron Transfer

DOI: 10.1002/anie.200905621

Electron Hopping over 100 Å Along an α Helix**

*Yoko Arikuma, Hidenori Nakayama, Tomoyuki Morita, and Shunsaku Kimura**

Electron transfer through biomolecules has been of great interest for the understanding of energy conversion and mass transduction in nature and for the development of molecular-based electronics.[1–15] In particular, the electron transfer in electron-transport proteins has been widely studied by spectroscopies with engineered proteins[7,14–16] and by electrochemistry with proteins immobilized on a metal surface.[12,13] More specifically, the electron transfer through α helices has attracted much attention because their parallel assemblies are a universal motif found in biological electron-transfer systems, and the helices are considered to play important roles in long-range electron transfer in proteins. Therefore, the electron transfer through model helical peptides has been extensively studied by various techniques in solution[1,17] and on metal surfaces.[18–22]

These studies have revealed interesting features: 1) a helical peptide is a good mediator of electron tunneling[17,21] compared to hydrocarbon chains;[23] 2) the helix macrodipole accelerates the electron transfer, as demonstrated in solution[24] and on a metal surface;[25] and 3) at longer distances beyond a critical molecular length, the electron-transfer mechanism switches from simple electron tunneling to another mechanism characterized by a very shallow distance dependence.[26,27] For the last feature, two mechanisms have been proposed: a hopping mechanism with the amide groups as hopping sites,[18,28] and molecular dynamics-associated electron tunneling.[19] Efficient hole hopping along bases in DNAs has been generally recognized.[4,5] Electron transfer through peptide nucleic acids (PNAs) has also been investigated[8–11] and the contribution of a hopping mechanism has been proposed.[9,10] On the other hand, despite of a lot of studies, the hopping contribution in peptide electron transfer still remains a matter of debate.[26–29]

In this study, we prepared well-defined self-assembled monolayers (SAMs)[30–33] on gold from helical peptides of different lengths from 8 mer to 64 mer, and studied the electron transfer through the helices electrochemically. We observed nonexponential distance dependence and high activation energies of the electron transfer, which suggest a hopping mechanism with the amide groups as hopping sites. This suggestion has been successfully validated by in-depth calculations taking tunneling and hopping into consideration. Importantly, the 64-mer helical peptide provides an electron path of over 100 Å along the helix and a regular monolayer of approximately 80 Å in thickness, in which electrons are exchanged at a significant rate constant of 0.5 s^{-1} for electron transfer through dielectric organic materials.

SAMs of redox-terminated helical peptides have been employed as ideal model systems to study the electron transfer through helical peptides.[18,19,22,27,34–36] We synthesized 8-, 16-, 32-, 48-, and 64-mer helical peptides carrying a lipoic acid for the linker to gold at the N terminus and a redox-active ferrocene unit at the C terminus (A8, A16, A32, A48, A64, respectively; Figure 1). The helix segment has an alternating sequence of L-alanine (Ala) and α-aminoisobutyric acid (Aib). The respective peptides were synthesized by the liquid-phase method, and their helical conformation was confirmed by circular dichroism (CD) spectroscopy in solution (see Figure S1 in the Supporting Information). Each peptide was immobilized on a gold surface through a gold–sulfur linkage to form a SAM by immersion of a gold substrate into the peptide solution.

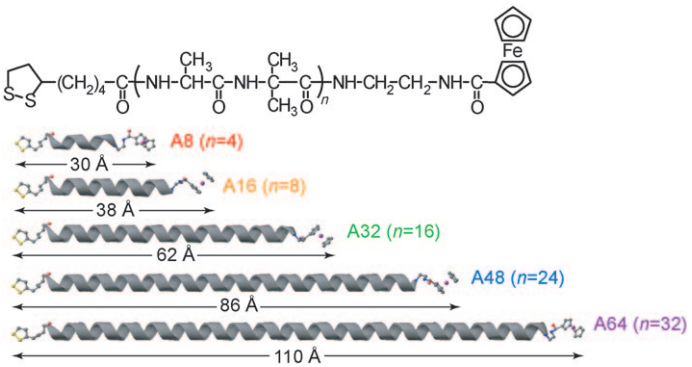

Figure 1. Chemical structures and schematic illustration of the helical peptides. The helices are expressed in a ribbon representation and the other atoms are shown in a ball-and-stick format: C gray; N blue; O red; S yellow; Fe purple.

First, we examined the molecular orientation by infrared reflection–absorption spectroscopy (IRRAS). The representative spectra are shown in Figure 2a. Amide I and II bands are observed at 1680–1670 and around 1540 cm^{-1}, respectively. The tilt angles of the helices from the surface normal (Figure 2a) were determined by comparing the experimental

[*] Y. Arikuma, H. Nakayama, Dr. T. Morita, Prof. S. Kimura
Department of Material Chemistry
Graduate School of Engineering, Kyoto University
Kyoto-Daigaku-Katsura, Nishikyo-ku, 615-8246 Kyoto (Japan)
Fax: (+81) 75-383-2401
E-mail: shun@scl.kyoto-u.ac.jp
Homepage: http://pixy.polym.kyoto-u.ac.jp/

[**] This work was financially supported by Grants-in-Aid for Young Scientists B (16750098), for Young Scientists A (20685009), for Exploratory Research (17655098), and for Scientific Research B (18350063, 21350061), and by the Global COE program, International Center for Integrated Research and Advanced Education in Materials Science, from the Ministry of Education, Culture, Sports, Science, and Technology (Japan).

Supporting information for this article is available on the WWW under http://dx.doi.org/10.1002/anie.200905621.

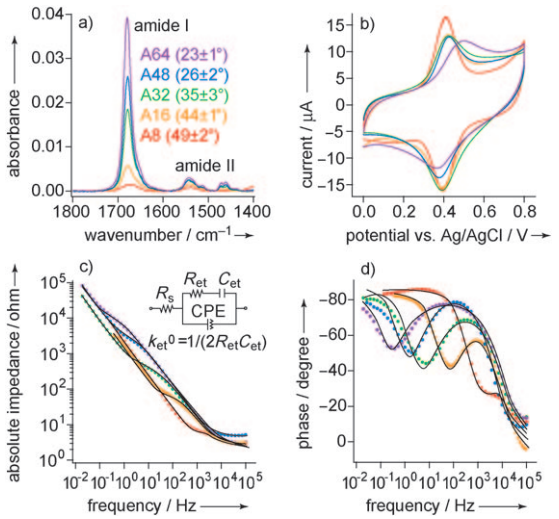

Figure 2. Results of IRRAS and electrochemical studies. a) Representative IRRAS spectra with the tilt angles in parentheses. The spectra are: A8 red, A16 orange, A32 green, A48 blue, and A64 purple. b) Cyclic voltammograms measured in aqueous 1 M $HClO_4$ at a scan rate of 0.1 $V s^{-1}$. c) Plot of absolute impedance versus frequency; the colored filled circles are the experimental data and the solid lines are the fitting curves. Inset: an equivalent circuit used for the analysis of the EIS results. CPE: constant-phase element. d) Plot of phase versus frequency with the fitting curves (solid lines).

spectra with simulated spectra[37] (Figure S2 in the Supporting Information). The tilt angles show that the helices become more vertical as the chain is elongated. This finding can be explained by stronger intermolecular interactions among the longer helices, which result in a more vertical orientation.[27] The experimental results for the monolayer thicknesses and the surface densities are consistent with the calculated results on the basis of the tilt angles (Table 1), thus indicating that the peptides form a well-packed monolayer with homogeneous orientation. To the best of our knowledge, the A64 SAM has a component of the highest and uniform molecular weight (5458.28 $g mol^{-1}$) and the largest thickness (77 Å) among the well-defined monolayers ever prepared. Blocking experiments in a ferrocyanide solution confirmed the well-packed property of the monolayers (Figure S3 in the Supporting Information).

To study the electron transfer from the ferrocene unit to gold, we performed cyclic voltammetry (CV) in a $HClO_4$ aqueous solution (Figure 2b). In all the SAMs, reversible redox peaks of ferrocenium/ferrocene are clearly observed, surprisingly even in the A64 SAM, thus showing that an electron is exchanged between the ferrocene unit and gold. The formal potentials are about 0.45 V in all the SAMs. The large peak separation in the cyclic voltammogram of the A64 SAM indicates that the electron transfer is on a comparable timescale to the scan rate (0.1 $V s^{-1}$). Notably, an electron is transferred from the ferrocene unit to gold over 100 Å along the helix at a timescale of subseconds.

Next, we carried out electrochemical impedance spectroscopy (EIS) at 0.45 V to determine the standard electron-transfer rate constants (k_{et}^0). The results are presented in Figure 2c and d in the form of Bode plots. The results were analyzed with an equivalent circuit[32] (inset in Figure 2c) to determine the k_{et}^0 values (Table 1). Figure 3a shows the semilog plot of k_{et}^0 versus the ellipsometry thickness. The nonlinear relationship in the semilog plot clearly indicates that the electron transfer through these helices is not governed by conventional electron tunneling, which should

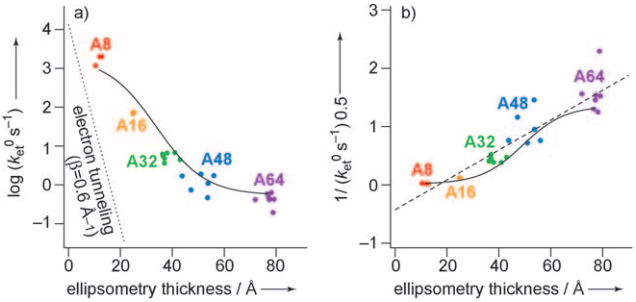

Figure 3. Distance dependence of k_{et}^0 on the monolayer thickness. a) Plot of the common logarithm of k_{et}^0 versus the monolayer thickness determined by ellipsometry. The colored filled circles are the experimental data, the dotted line is the reference curve of electron tunneling with a decay constant of 0.6 $Å^{-1}$, and the solid line shows the result of calculations upon taking the tunneling and hopping mechanisms into consideration. b) Plot of the inverse of the square root of k_{et}^0 versus the ellipsometry thickness. The dashed line is the linear fit and the solid line shows the result of calculations upon taking the tunneling and hopping mechanisms into consideration.

Table 1: Summary of this work.

SAM	A8	A16	A32	A48	A64
tilt angle[a] [°]	49.4 ± 1.6	43.7 ± 0.8	35.0 ± 3.1	26.2 ± 2.4	23.1 ± 1.3
calculated monolayer thickness[b] [Å]	10.4 ± 0.3	17.4 ± 0.2	39.3 ± 1.5	64.6 ± 1.4	88.3 ± 0.9
experimental monolayer thickness[c] [Å]	11.7 ± 1.3	24.9 ± 0.2	38.4 ± 2.6	50.9 ± 4.6	77.1 ± 2.4
calculated surface density[b] ($\times 10^{-11}$) [$mol cm^{-2}$]	14.0 ± 0.4	11.9 ± 0.2	13.5 ± 0.5	14.8 ± 0.3	15.2 ± 0.2
experimental surface density[d] ($\times 10^{-11}$) [$mol cm^{-2}$]	17.3 ± 2.0	15.1 ± 3.9	13.5 ± 0.6	11.1 ± 1.6	10.2 ± 2.1
experimental k_{et}^0 at 298 K[e] [s^{-1}]	1725 ± 475	71.5 ± 3.6	5.43 ± 1.13	1.28 ± 0.59	0.45 ± 0.15
calculated k_{et}^0 ($k_{hop} + k_{tun}$) at 298 K [s^{-1}]	899.76	195.36	11.39	1.77	0.58
calculated k_{hop} (hopping) at 298 K [s^{-1}]	887.73	195.26	11.39	1.77	0.58
calculated k_{tun} (tunneling) at 298 K [s^{-1}]	12.02	0.10	5.5×10^{-8}	3.1×10^{-14}	1.7×10^{-20}
experimental activation energy[e] [eV]	0.42 ± 0.01	0.40 ± 0.01	0.36 ± 0.03	0.45 ± 0.11	0.51 ± 0.12
calculated activation energy [eV]	0.382	0.418	0.496	0.545	0.570

[a] Determined by IRRAS. [b] Calculated from the IRRAS tilt angles and helix lengths or cross-sectional areas. [c] Determined by ellipsometry. [d] Estimated by integration of anodic peaks in the cyclic voltammograms after subtraction of the background current. [e] Determined by EIS.

show a linear relationship with a slope of the decay constant (β).[23] For reference, a linear distance dependence of electron tunneling is also shown as a dotted line in Figure 3a with an assumption for β[17,21] of 0.6 Å^{-1}, which is too steep to explain the present data. On the other hand, in a hopping mechanism, the rate constant is inversely proportional to the square of the distance if the energies of the hopping sites are identical and hopping is reversible about the direction.[38]

Figure 3b shows the plot of the inverse of the square root of k_{et}^0 versus the distance. A roughly linear relationship among the peptides used here is observed (dashed line), further supporting our interpretation of the hopping mechanism for electron transfer. We also determined the activation energies by variable-temperature measurements (Figure S4 in the Supporting Information, Table 1). If electron tunneling is operative, the activation energy is about 0.2 eV, which is one fourth of the reported reorganization energy of a ferrocene moiety.[32] The observed activation energies that are significantly larger than 0.2 eV also suggest a contribution of the hopping mechanism to the electron transfer. The plausible hopping sites are the amide groups and it is likely that a hole hops among the amide groups when taking the frontier-orbital levels of an amide group into consideration, that is, the HOMO of the amide is close to the Fermi level.[36] Therefore, an electron is first transferred from the N-terminal amide group to gold to generate the cation radical of the amide group, the cation radical hops among the amide groups to reach the C terminus, and finally it is reduced by the ferrocene unit, which completes the overall electron transfer from the ferrocene unit to gold (Figure 4b).

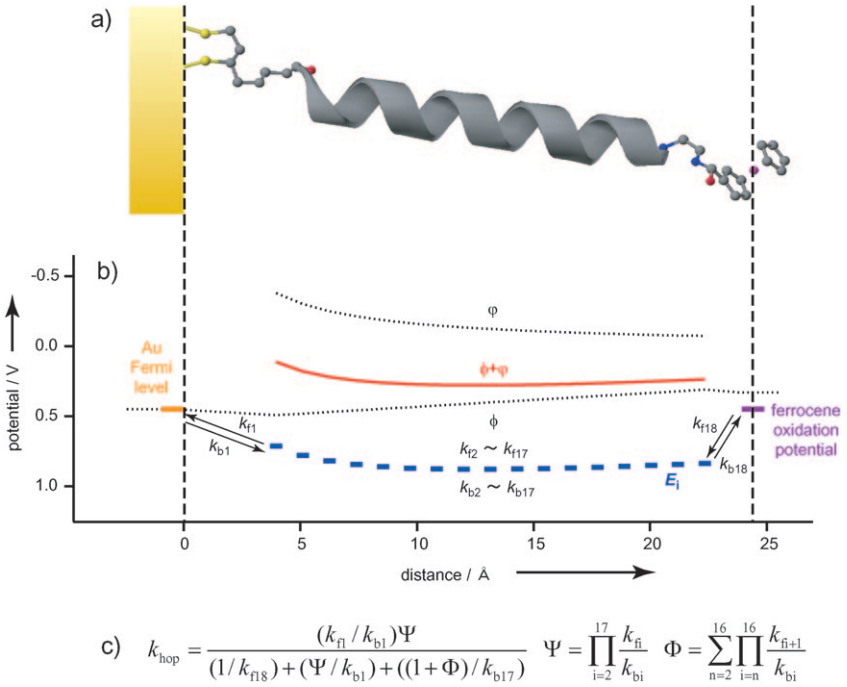

Figure 4. Calculation of k_{et}^0 in the A16 SAM. a) The A16 SAM. b) Results of the calculations of electrostatic potential (ϕ), stabilization energy by image-dipole formation (φ), and the oxidation potentials of the amide groups in the monolayer (E_i, i=2–18). k_{fi} and k_{bi} are the rate constants of forward and backward electron tunneling between the ith and (i+1)th sites, respectively. c) Ratner's formalism used for the calculation of k_{et}^0 by the hopping mechanism.

To quantitatively discuss the results, calculations of k_{et}^0 were carried out (see the Supporting Information for details). k_{et}^0 is the sum of the rate constants of the electron tunneling and the hopping mechanism. The rate constants of electron tunneling were calculated by a formalism for interfacial molecule–metal electron transfer.[30] On the other hand, the rate constants for the hopping mechanism were determined as follows. First, the electrostatic-potential profiles in the monolayer and the stabilization energies of the amide cation radicals from the image dipole formed inside the metal were calculated. The oxidation potential of an amide group in a peptide chain was determined by CV in dimethylformamide (DMF; Figure S5 in the Supporting Information). Solvent oxidation currents were properly subtracted in the voltammograms. Three different peptide samples (Boc-(Ala-Aib)$_4$-OBzl, Boc-(Ala-Aib)$_4$-OH, and Boc-(Ala-Aib)$_8$-OBzl; Boc = *tert*-butoxycarbonyl, Bzl = benzyl) showed similar redox peaks, whereas Boc-Ala-OH without an amide group did not show the peaks, thus indicating that the observed redox peaks originate from the oxidation of the amide groups. The oxidation potential was determined to be 0.93 V versus Ag/AgCl. This rather surprisingly low oxidation potential can be explained by stabilization of the amide cation radical by neighboring amide groups in a peptide chain,[29] delocalization over a few amide groups, or more specific interactions between neighbors, such as three-electron bond formation, which has been recently proposed as a hole carrier in a peptide chain.[39]

From this oxidation potential along with the electrostatic potential and image-dipole stabilization energies, the amide oxidation potentials in the SAMs were determined. A typical example of the A16 SAM is depicted in Figure 4b. The dipole moment of the helix was taken into account by locating partial charges at the termini. From these oxidation potentials, the rate constants of the respective electron-tunneling steps were calculated by formalisms for inhomogeneous molecule–metal[30] and homogeneous molecule–molecule[40] electron transfer. The rate constant of hole transfer among the amide groups was calculated to be on the order of 10^{10} s^{-1}. Finally, by using these rate constants, the overall rate constants were calculated by Ratner's formalism[38] (Figure 4c).

The calculated k_{et}^0 values are summarized in Table 1 and the calculated curves are shown in Figure 3a and b as solid lines. The calculations excellently reproduce the experimental k_{et}^0 values. It is found that the hopping mechanism is dominant in all the SAMs. Previously, we speculated that electron tunneling prevailed in the 8-mer SAM simply because of the relatively large decay constant,[27] but the

hopping mechanism is found here to be dominant even in the 8-mer SAM.

The activation energies (Table 1) are also calculated from theoretical k_{et}^0 values at 298 and 323 K. They are consistent with the experimental values, and are significantly larger than those of the tunneling case. Reasonably, the activation energies are found to correspond to the energy gaps between the gold Fermi level and the oxidation potential of the amide group, which shows the most positive value in the energy diagram (Tables S1–S5 in the Supporting Information). The good agreement of the theoretical and experimental data indicates that the hopping mechanism is responsible for the long-range electron transfer, and accordingly the electron transfer is persistent over long distances with measurable electron-transfer rate constants. Most importantly, an electron is transferred over 100 Å along the 64-mer helical peptide at a moderate rate constant of 0.5 s^{-1}. To the best of our knowledge, this is the longest-range electron transfer through a molecule ever investigated with a rate constant determined.

Molecular-dynamics-associated or conformational-gating electron tunneling has been proposed to explain a shallow distance dependence, in which a peptide chain thermally fluctuates to reach an active conformer enabling efficient electron tunneling.[19] However, it is unlikely that a helix shrinks, bends, or tilts to a large extent to reduce the electron-transfer distance down to an electron-tunneling range in a well-packed monolayer, especially for the present long helices with parallel arrangement. Therefore, a simple picture of molecular dynamics with global motions cannot explain our results. However, the conformational dynamics mechanism is still a possible explanation, setting aside the quantitative discussions on the rate constants, distance dependence, and activation energies, if there is a fraction of helices that can move freely near monolayer defects and whose ferrocene moiety is oxidized by conformational-gating electron tunneling, and then the other ferrocene moieties of the surrounding helices are oxidized through such active spots by hole migration among the ferrocene moieties.

Recent theoretical studies have shown that thermal structural fluctuations are important to dictate biological long-range electron-transfer reactions,[9,41,42] not only for superexchange mechanisms but also for charge-hopping mechanisms. Actually, our group has observed the effect of molecular motions on the electron transfer through long helical peptides, and proposed that local motions of peptide backbones promote hole hopping among the amide groups.[35] It has been theoretically proposed that conformational changes of a peptide chain facilitate hole hopping along the chain by significant enhancement of the electronic coupling and reduction of the activation energy.[29]

This work has implications for biological electron transfer and molecular-based electronics. Contributions of hopping among side chains of aromatic amino acids in electron transfer through model helical peptides[43] and long-range electron transfer in proteins[7,16,44] have been demonstrated. In these systems, the energy difference between the donor and the neighboring hopping site is less than 0.1 eV. On the other hand, in the present systems, the energy difference between the gold Fermi level and the oxidation potential of the neighboring amide group is about 0.3 eV (Tables S1–S5 in the Supporting Information). This larger energy difference causes the shift of the crossover distance of tunneling and hopping to a longer distance, which, however, turned out to be shorter than the shortest 8-mer peptide in the present case. This work also suggests that the intrinsic peptide backbone can serve as stepping stones. Hopping among amide groups might be involved in some long-range electron transfer if oxidation or reduction of the amide groups is energetically available. For application aspects, ferrocene-terminated helical-peptide monolayers can be used as unique interfaces between electron-transfer proteins and gold, in which the proteins can be immobilized while retaining their natural structure, and long-range electron communication between gold, ferrocene, and redox groups in the proteins is ensured. Such hybrid molecular systems sound promising for efficient solar-energy conversion, artificial catalysis, and biosensing.

Experimental Section

The helical peptides were synthesized by the liquid-phase method and identified by ^{1}H NMR spectroscopy and mass spectrometry (FAB and/or MALDI-TOF). Their purity was confirmed by HPLC to be $>98\%$. CD spectra of the peptides were measured on a CD spectropolarimeter in trifluoroethanol at $0.8–1.7\times10^{-3}$ M residue concentration at room temperature. SAMs were prepared by immersion of a gold substrate into solutions of the peptides in ethanol (A8 and A16) or ethanol/chloroform (A32, A48, and A64) at a concentration of approximately 1.0×10^{-4} M for 24 h. IRRAS was carried out on a Fourier transform infrared spectrometer with a reflection attachment at room temperature at an 84° incident angle from the surface normal. Ellipsometry was performed by an autoellipsometer at room temperature with a 632.8 nm He–Ne laser at a 65° incident angle, and the complex optical constant of the monolayer was assumed to be $1.50+0.00i$ in the thickness calculations. CV and EIS in aqueous 1 M $HClO_4$ were performed by voltammetric analyzers with a three-electrode system consisting of the monolayer-modified gold substrate (working), Ag/AgCl in aqueous NaCl (reference), and a platinum wire (counter). EIS was carried out at 0.45 V with a dc voltage of 10 mV at frequencies from 10^5 to 10^{-1} or 10^{-2} Hz. CV of the peptide solutions (ca. 0.8 mg mL^{-1}) was performed in a solution of 0.01 M tetrabutylammonium hexafluorophosphate in DMF with a gold disk electrode, Ag/Ag^+ in a 0.1 M tetrabutylammonium perchlorate solution in acetonitrile, and with a platinum wire. Molecular modeling was performed on semiempirical molecular orbital calculation software, and theoretical IRRAS spectra and electron-transfer rate constants were calculated by mathematical software. Full details of the experimental and theoretical methods are given in the Supporting Information.

Received: October 7, 2009
Revised: December 4, 2009
Published online: February 12, 2010

Keywords: electrochemistry · electron transfer · helical structures · monolayers · peptides

[1] S. S. Isied, M. Y. Ogawa, J. F. Wishart, *Chem. Rev.* **1992**, *92*, 381–394.
[2] D. N. Beratan, J. N. Onuchic, J. R. Winkler, H. B. Gray, *Science* **1992**, *258*, 1740–1741.

[3] M. R. Wasielewski, *Chem. Rev.* **1992**, *92*, 435 – 461.
[4] S. O. Kelley, J. K. Barton, *Science* **1999**, *283*, 375 – 381.
[5] M. Bixon, B. Giese, S. Wessely, T. Langenbacher, M. E. Michel-Beyerle, J. Jortner, *Proc. Natl. Acad. Sci. USA* **1999**, *96*, 11713 – 11716.
[6] S. M. Lindsay, M. A. Ratner, *Adv. Mater.* **2007**, *19*, 23 – 31.
[7] C. Shih, A. K. Museth, M. Abrahamsson, A. M. Blanco-Rodriguez, A. J. Di Bilio, J. Sudhamsu, B. R. Crane, K. L. Ronayne, M. Towrie, A. Vlcek, J. H. Richards, J. R. Winkler, H. B. Gray, *Science* **2008**, *320*, 1760 – 1762.
[8] A. Paul, R. M. Watson, P. Lund, Y. J. Xing, K. Burke, Y. F. He, E. Borguet, C. Achim, D. H. Waldeck, *J. Phys. Chem. C* **2008**, *112*, 7233 – 7240.
[9] E. Hatcher, A. Balaeff, S. Keinan, R. Venkatramani, D. N. Beratan, *J. Am. Chem. Soc.* **2008**, *130*, 11752 – 11761.
[10] B. Armitage, D. Ly, T. Koch, H. Frydenlund, H. Orum, H. G. Batz, G. B. Schuster, *Proc. Natl. Acad. Sci. USA* **1997**, *94*, 12320 – 12325.
[11] A. Paul, S. Bezer, R. Venkatramani, L. Kocsis, E. Wierzbinski, A. Balaeff, S. Keinan, D. N. Beratan, C. Achim, D. H. Waldeck, *J. Am. Chem. Soc.* **2009**, *131*, 6498 – 6507.
[12] A. Avila, B. W. Gregory, K. Niki, T. M. Cotton, *J. Phys. Chem. B* **2000**, *104*, 2759 – 2766.
[13] K. Fujita, N. Nakamura, H. Ohno, B. S. Leigh, K. Niki, H. B. Gray, J. H. Richards, *J. Am. Chem. Soc.* **2004**, *126*, 13954 – 13961.
[14] D. N. Beratan, J. N. Betts, J. N. Onuchic, *Science* **1991**, *252*, 1285 – 1288.
[15] R. Langen, J. L. Colon, D. R. Casimiro, T. B. Karpishin, J. R. Winkler, H. B. Gray, *J. Biol. Inorg. Chem.* **1996**, *1*, 221 – 225.
[16] H. B. Gray, J. R. Winkler, *Chem. Phys. Lett.* **2009**, *483*, 1 – 9.
[17] M. Sisido, S. Hoshino, H. Kusano, M. Kuragaki, M. Makino, H. Sasaki, T. A. Smith, K. P. Ghiggino, *J. Phys. Chem. B* **2001**, *105*, 10407 – 10415.
[18] T. Morita, S. Kimura, *J. Am. Chem. Soc.* **2003**, *125*, 8732 – 8733.
[19] H. B. Kraatz, I. Bediako-Amoa, S. H. Gyepi-Garbrah, T. C. Sutherland, *J. Phys. Chem. B* **2004**, *108*, 20164 – 20172.
[20] X. Y. Xiao, B. Q. Xu, N. J. Tao, *J. Am. Chem. Soc.* **2004**, *126*, 5370 – 5371.
[21] S. Sek, A. Misicka, K. Swiatek, E. Maicka, *J. Phys. Chem. B* **2006**, *110*, 19671 – 19677.
[22] J. J. Wei, C. Schafmeister, G. Bird, A. Paul, R. Naaman, D. H. Waldeck, *J. Phys. Chem. B* **2006**, *110*, 1301 – 1308.
[23] J. F. Smalley, H. O. Finklea, C. E. D. Chidsey, M. R. Linford, S. E. Creager, J. P. Ferraris, K. Chalfant, T. Zawodzinsk, S. W. Feldberg, M. D. Newton, *J. Am. Chem. Soc.* **2003**, *125*, 2004 – 2013.
[24] E. Galoppini, M. A. Fox, *J. Am. Chem. Soc.* **1996**, *118*, 2299 – 2300.
[25] S. Yasutomi, T. Morita, Y. Imanishi, S. Kimura, *Science* **2004**, *304*, 1944 – 1947.
[26] R. A. Malak, Z. N. Gao, J. F. Wishart, S. S. Isied, *J. Am. Chem. Soc.* **2004**, *126*, 13888 – 13889.
[27] M. Kai, K. Takeda, T. Morita, S. Kimura, *J. Pept. Sci.* **2008**, *14*, 192 – 202.
[28] E. G. Petrov, Y. V. Shevchenko, V. I. Teslenko, V. May, *J. Chem. Phys.* **2001**, *115*, 7107 – 7122.
[29] E. W. Schlag, S. Y. Sheu, D. Y. Yang, H. L. Selzle, S. H. Lin, *Angew. Chem.* **2007**, *119*, 3258 – 3273; *Angew. Chem. Int. Ed.* **2007**, *46*, 3196 – 3210.
[30] C. E. D. Chidsey, *Science* **1991**, *251*, 919 – 922.
[31] H. O. Finklea, D. D. Hanshew, *J. Am. Chem. Soc.* **1992**, *114*, 3173 – 3181.
[32] S. E. Creager, T. T. Wooster, *Anal. Chem.* **1998**, *70*, 4257 – 4263.
[33] J. C. Love, L. A. Estroff, J. K. Kriebel, R. G. Nuzzo, G. M. Whitesides, *Chem. Rev.* **2005**, *105*, 1103 – 1169.
[34] S. Sek, A. Tolak, A. Misicka, B. Palys, R. Bilewicz, *J. Phys. Chem. B* **2005**, *109*, 18433 – 18438.
[35] K. Takeda, T. Morita, S. Kimura, *J. Phys. Chem. B* **2008**, *112*, 12840 – 12850.
[36] Y. Arikuma, K. Takeda, T. Morita, M. Ohmae, S. Kimura, *J. Phys. Chem. B* **2009**, *113*, 6256 – 6266.
[37] R. Schwyzer, P. Moutevelis-Minakakis, S. Kimura, H. U. Gremlich, *J. Pept. Sci.* **1997**, *3*, 65 – 81.
[38] Y. A. Berlin, M. A. Ratner, *Radiat. Phys. Chem.* **2005**, *74*, 124 – 131.
[39] X. H. Chen, L. Zhang, Z. P. Wang, J. L. Li, W. Wang, Y. X. Bu, *J. Phys. Chem. B* **2008**, *112*, 14302 – 14311.
[40] R. A. Marcus, N. Sutin, *Biochim. Biophys. Acta Rev. Bioenerg.* **1985**, *811*, 265 – 322.
[41] A. A. Voityuk, *J. Chem. Phys.* **2008**, *128*, 115101.
[42] F. C. Grozema, S. Tonzani, Y. A. Berlin, G. C. Schatz, L. D. A. Siebbeles, M. A. Ratner, *J. Am. Chem. Soc.* **2008**, *130*, 5157 – 5166.
[43] B. Giese, M. Wang, J. Gao, M. Stoltz, P. Muller, M. Graber, *J. Org. Chem.* **2009**, *74*, 3621 – 3625.
[44] C. S. Yee, M. R. Seyedsayamdost, M. C. Y. Chang, D. G. Nocera, J. Stubbe, *Biochemistry* **2003**, *42*, 14541 – 14552.

